JOURNAL OF GUIDANCE, CONTROL, AND DYNAMICS
Vol. 26, No. 4, July–August 2003

Lunar Gravitational Capture Conditions

Scott R. Dahlke*
U.S. Air Force Academy, U.S. Air Force Academy, Colorado 80840

Certain classes of lunar trajectories allow spacecraft to approach the moon from outside its sphere of influence and to end up in a temporarily captured state around the moon without any thrusting necessary. The spacecraft's state at the moon associated with these efficient types of capture is investigated. First, analysis is done on objects approaching the moon from a direction that results in the lowest eccentricity at perilune. Following that, analysis is done on objects approaching the moon with trajectories that originate from the Earth. This second set of orbits are ballistic capture transfer trajectories that allow spacecraft to go from low Earth orbit to lunar capture with only one engine burn at Earth. The properties investigated provide insight to this particular form of transfer and can help in mission design.

Introduction

A SET of trajectories called ballistic capture transfer (BCT) trajectories (Fig. 1) is one of the most fuel-efficient methods of putting a spacecraft in orbit around the moon.[1–4] Through the use of third-body perturbations, only one maneuver (ΔV) is necessary to go from low Earth orbit to a point where the satellite is in a captured or elliptical orbit around the moon. Note that this lunar capture is only temporary. The spacecraft approaches the moon with hyperbolic velocity, but third-body perturbations from the sun and Earth decrease the energy level to the point that the orbit is elliptical when it arrives at the moon. However, these same perturbations will eventually cause the spacecraft to gain energy and escape from the moon's influence. The length of the capture time is discussed later in this paper.

Although all of the BCT trajectories analyzed for this study look similar to the trajectory in Fig. 1, there are several other families of BCTs with lunar swing-by, multiple revolutions around the Earth, and other distinguishing characteristics. The family of BCTs studied here is faster and more fuel-efficient than most of the other BCT families.

In practice, it is difficult to design one of these ballistic capture transfers that departs the Earth and arrives at the moon within a captured state. The initial trajectory conditions that approach the moon in a capture-type situation are highly nonlinear and, therefore, very elusive in the design process. Consequently, much of the work done with these trajectories has been accomplished by starting at the moon with the desired lunar orbital elements. Then the orbit is propagated backward in time with different initial velocities until an orbit is found that just barely escapes the moon, travels to near the Earth–sun sphere of influence, and then drops back to pass very close to the Earth.[4]

The first step is to pick the initial state, usually fixing the radius of perilune and inclination desired. In this study, the velocity vector is perpendicular to the position vector and parallel to the ecliptic plane. The other elements are set such that the perilune point is situated on the Earth side of a line connecting the Earth and the moon (Fig. 2). This initial configuration was shown to be optimal from the viewpoint that, here, the spacecraft is at the most strongly captured point, but that when propagated backward in time, it will still result in an escape from the moon.[2]

The reason that this is an optimal location for the perilune point is because of the direction from which the spacecraft approaches the moon. Yamakawa et al.[5] show that for the Earth, moon, and spacecraft three-body problem, the spacecraft will lose energy with respect to the moon if the spacecraft approaches from certain directions. Figure 3 shows those approximate directions as shaded regions and also has a typical approach from a BCT trajectory. Note that the coordinate frame is rotating with the Earth/moon line.

Eccentricity is set at some arbitrarily large value, 0.85 for example, and the orbit is propagated backward in time. If the spacecraft does not escape the moon, then the state is varied until a minimum eccentricity value is found that allows the spacecraft to escape. Because of third-body effects (mainly from the Earth) and the location at which the spacecraft starts, the spacecraft will usually escape the moon with an initial eccentricity of less than one.

Once an escape orbit is found, eccentricity is increased by very small amounts to find an orbit that travels beyond the Earth–sun sphere of influence (approximately 925,000 km) and back to Earth. Variation of eccentricity by this small amount will usually result in an orbit that does approach the Earth. The orbits that do pass close to Earth are then BCT trajectories when propagated forward from Earth. Whether the trajectory comes near the Earth or not is primarily dependent on the direction of the sun when the satellite is near apogee.

Because the trajectories are starting at the moon and are being propagated backward in time, the conditions at the moon associated with BCTs are the focus of this paper. Previous work has been done to determine the optimal placement of the perilune when trying to achieve a ballistic capture.[2,5,6] These studies indicate that the perilune location should be placed near a line between the moon and the Earth. However, the work presented here expands on that by exploring the characteristics of ballistic captures for various sun–Earth–moon configurations. This sun–Earth–moon relationship is important to the problem because the perturbations of the various bodies are what make the BCT trajectory possible.

After preliminary definitions and data descriptions, lunar escape velocities are presented and analyzed. These are followed by BCT velocities, which are close to the escape velocities. However, instead of just escaping the moon, they are given just enough extra velocity to travel beyond the Earth's sphere of influence and then return to pass the Earth at an altitude of 200 km. Note that all of these are found with backward time propagation. By the use of this BCT velocity information, further analysis is presented indicating the conditions that are best for BCT trajectories, how stable the lunar captures are, and the path on which BCT trajectories approach the moon.

Sun–Earth–Moon Angle

Many parameters that are studied have repetitive patterns with a period of about 29.5 days, roughly one lunar synodic month. This synodic month is defined as the time from one new moon to the next new moon. To help analyze this periodic effect, an angle is defined that will be used as an independent variable in some of the cases.

Received 9 December 1999; revision received 10 February 2003; accepted for publication 18 February 2003.

*Associate Professor, Department of Astronautics. Associate Fellow AIAA.

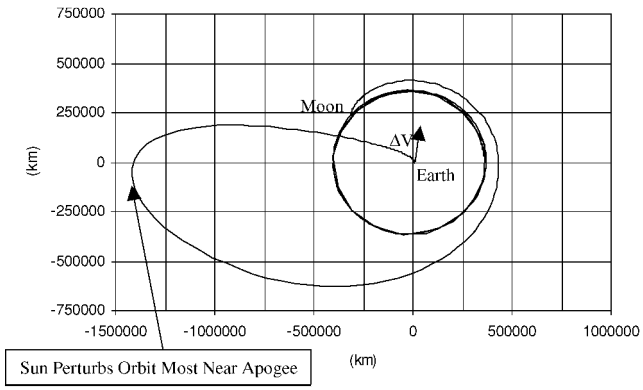

Fig. 1 BCT (Earth-centered inertial frame).

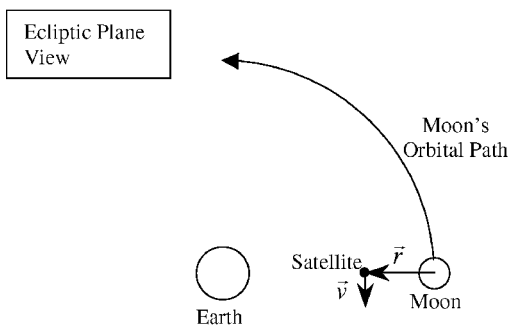

Fig. 2 Initial conditions for backward propagation.

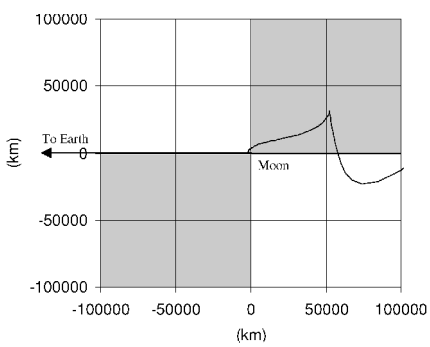

Fig. 3 Spacecraft lunar approach (Earth/moon rotating coordinates).

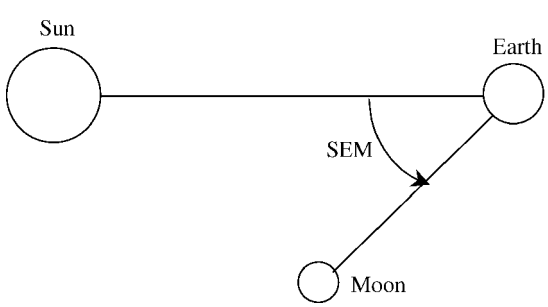

Fig. 4 Definition of SEM angle.

This angle is the difference between the mean longitude of the moon and the mean longitude of the sun (Fig. 4). The mean longitude is measured along the ecliptic, to the mean ascending node, and then along the mean orbit.

This will be referred to as the sun–Earth–moon (SEM) angle in this paper, but it is sometimes called the mean elongation of the moon from the sun. The secular changes can be approximated with the following formula[7]:

$$\text{SEM} = 32.508133\ \text{deg} + 12.19074912d \tag{1}$$

Several of the equations presented are written as functions of a parameter d. This parameter d is the number of days that have elapsed since 0000 hrs 1 January 1998. It can be computed with the Julian date (JD)

$$d = \text{JD} - 2450814.5$$

At points in the analysis, it will be desirable to compute a JD given a specific SEM angle. There is not a unique solution due to the periodic nature of this function because solutions occur about every 29.5 days:

$$d = \frac{\text{SEM} - 32.508133}{12.19074912} \pm k29.530589 \tag{2}$$

where k is an integer.

Description of Orbit Data for Analysis

For the analysis in this paper, many ballistic capture trajectories are found starting with various initial SEM angles. The way various angles are obtained is by starting at different epochs. As the epoch changes, so does the SEM angle. The rate at which this angle changes is close to 360 deg in 1 lunar month, or approximately 12 deg per day. When several trajectories over the span of one lunar month are found, the 360-deg range of the SEM angles can be analyzed. However, to see how repeatable resulting patterns are from one cycle to the next, several ballistic capture trajectories were found over a large time span.

The set of orbits used for analysis have a wide range of epochs from which the orbits are propagated backward. The primary data set contains perilune epochs that start at 0000 hrs, 1 January 1998 and are spaced at one-day intervals over a four-year time span. Only a portion of the data set is shown so that variations in the parameter of interest can be seen easily.

In addition to the study over a wide range of epochs, several perilune altitudes were studied. This was done to determine if the effects observed were valid for several different final orbit sizes. An altitude of 100 km is used for the primary analysis in each section, but other altitude results are presented following that.

To propagate the orbits backward, a Runge–Kutta 7(8) integrator is used in conjunction with a model that includes accelerations due to the sun, Earth, moon, and the J_2 effects caused by the Earth's oblate shape.

Lunar Escape/Capture Conditions

There are some interesting aspects to the lunar arrival conditions, or, equivalently, to the lunar departure conditions, when work is done backward in time. In this section, BCT trajectories are not considered yet, but instead the minimum amount of velocity needed to escape from the moon is studied.

First of all, a comparison can be done between the two-body escape velocity from the moon and the actual escape velocity as determined from numerical integration. From the two-body equations, the escape velocity of the moon should be

$$v_{\text{esc2}} = \sqrt{2\mu_m / r_m} \tag{3}$$

where v_{esc2} is the two-body escape velocity from the moon at a 100-km altitude, μ_m is the gravitational parameter of the moon (4902.8 km^3/s^2), and r_m is the distance of the spacecraft from the center of the moon (1838 km).

For the nominal lunar altitude used here (100 km), the escape velocity is approximately 2.3097 km/s. This is then compared to many actual escape velocities found from the moon over a span of one year using the numerical integration results (Fig. 5).

The actual escape velocities are all 40–45 m/s below the two-body escape velocities. Therefore, for all of the cases in Fig. 5, the orbits are elliptical with respect to the moon at the perilune point, but the apoapsis is large enough that perturbations allow an escape to occur. The trajectories here are similar to the trajectory in Fig. 3,

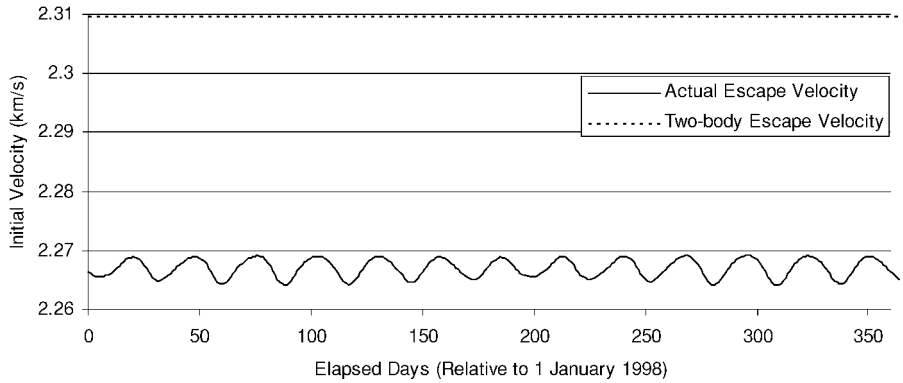

Fig. 5 Lunar escape velocity (two-body vs actual).

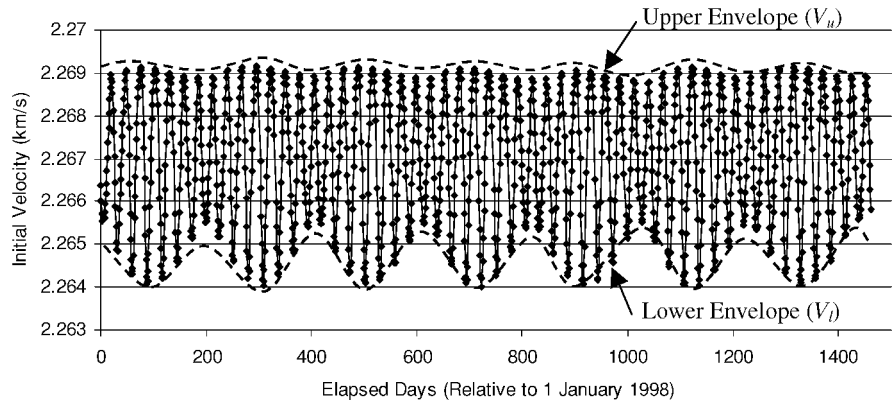

Fig. 6 Actual escape velocity for four years.

where the trajectory approaching the moon looses energy. Here, the trajectory is being propagated backward in time so that energy is being gained. From Fig. 5, a 13 cycle per year pattern can be seen in the actual escape velocity, which is close to the length of a lunar month. Figure 6 is the actual escape velocity v_{esc} plotted again, except that this time the vertical scale has been adjusted to show more detail, and the time span has been expanded to four years.

With this new scale and four-year time span, note that, in addition to the roughly 28-day cycle, there is also a long-term variation that is superimposed on it. To determine better estimates of these periods, a model is developed and then fit to the data. First an upper and lower "envelope" boundary is defined, as in Fig. 6. Then the 28-day period is fit inside this.

An oscillatory behavior can be described as

$$V_{\text{esc}} = A_s(t)\cos[(d + P_s)2\pi/T_s] + B_s(t) \tag{4}$$

where $A_s(t) = (V_u - V_l)/2$, P_s is the phase offset, T_s is the period of the short term oscillations, and $B_s(t) = (V_u + V_l)/2$.

Because the amplitude and bias of the oscillations vary with time, models for these terms are also defined. They are formed from functions of the upper and lower envelope boundaries.

$$V_u = A_u\cos[(d + P_u)2\pi/T_u] + B_u$$

$$V_l = A_l\cos[(d + P_l)2\pi/T_l] + B_l \tag{5}$$

where V_u and V_l model the upper and lower envelope boundaries, respectively; P_l and P_u are phase offsets of the upper and lower envelopes (opposite phases assumed); and T_u are T_l are the period of the envelope oscillations (assumed to be equal).

With the preceding model, the escape velocity data from Fig. 6 are used to generate a best fit using a nonlinear least-squares method. The result of this fit is as follows:

$$A_u = 0.0003720031041\,\text{km/s}$$

$$A_l = 0.0003865526712\,\text{km/s}$$

$$P_s = 7.815448604\,\text{days}$$

$$P_u = 109.5080397\,\text{days}$$

$$P_l = P_u + \tfrac{1}{2}T_u = 212.5141362\,\text{days}$$

$$T_s = 27.55833503\,\text{days}$$

$$T_u,\ T_l = 206.0121929\,\text{days}$$

$$B_u = 2.269081482\,\text{km/s}$$

$$B_l = 2.264848265\,\text{km/s}$$

With these best-fit values, more in-depth analysis can be performed on the variations. The first and largest effect to investigate consists of the short-term oscillations identified earlier as having a period of about 28 days. A more accurate value for this oscillation period comes from the preceding T_s value, which has a best-fit value of 27.55833503 days. This corresponds very closely with the lunar anomalistic month (perigee to perigee) of 27.554550 days (Ref. 7). Thus, the short-period variations correspond with how close the moon is to the Earth.

From the $\cos[(d + P_s)2\pi/T_s]$ portion of the V_{esc} formula, it can be determined that the least expensive times to do a ΔV in this 27.55-day cycle are when the cosine term is at its minimum (or -1.0). Solving this results in minima occurring at

$$d_{\min} = 5.963718911 + 27.55833503k \tag{6}$$

where $d_{\min}$ is the elapsed days from 0000 hrs, 1 January 1998, of the minimum values, and k is an arbitrary integer. Because the period is the same at the anomalistic month, the location of the minimum ΔV always occurs at the same true anomaly of the moon's orbit about the Earth.

The Astronomical Almanac has several equations describing the motion of the moon, but none of them give the true anomaly of the

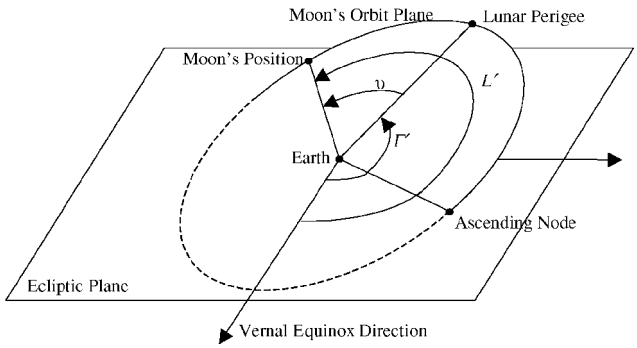

Fig. 7 Angles involved in computing lunar true anomaly.

moon directly, and so equations must be combined. Figure 7 depicts the angles that will be used to derive the moon's true anomaly.

The first angle is the mean longitude of the moon. The mean longitude of the moon L' is measured in the ecliptic to the mean ascending node and then along the mean orbit. The next parameter of use is the mean longitude of lunar perigee. The mean longitude of the lunar perigee Γ' is measured in the ecliptic to the mean ascending node and then along the mean orbit to the perigee direction.

The true anomaly of the moon can be computed by differencing the mean longitude of the moon and the mean longitude of lunar perigee. By the use of equations from the 1998 Astronomical Almanac,

$$v_m = L' - \Gamma' = 310.985637\,\text{deg} + 13.06499294\,d \qquad (7)$$

When the true anomaly is set equal to 360 deg and d is solved, the elapsed number of days into 1998 can be computed for the first lunar perigee. Therefore, lunar perigees occur on dates according to the following equation:

$$d_{\text{pm}} = 3.751579754 + 27.554550k \qquad (8)$$

where d_{pm} are the dates that the moon is at perigee relative to 0000 hrs, 1 January 1998, and k is an arbitrary integer.

Note that this equation has been derived from the mean longitude of the moon and the mean longitude of the lunar perigee, and so periodic variations have been ignored. Therefore, the dates of the lunar perigees will not necessarily coincide exactly with the dates provided by this equation.

By comparison of Eqs. (6) and (8), note that the minimum ΔV location in the lunar orbit occurs 2.21213916 days after lunar perigee. Given a constant angular rate and a lunar period of 27.554550 days, the corresponding lunar true anomaly is 28.90158241 deg. In other words, to arrive at the moon with the lowest amount of energy, the arrival should occur when the moon is at a true anomaly of 28.9 deg.

This result is not surprising when the work done by Neto and Prado[8] is considered. They studied the most efficient lunar capture/escape conditions for the elliptical restricted three-body problem. Their conclusion was that the most efficient location to do the capture/escape is when the moon has a true anomaly near 0 deg. However, they only investigated the cases at 90-deg increments: 0, 90, 180, and 270 deg. Because of this, the most efficient true anomaly could exist in the range from 0 to 45 deg or 315 to 360 deg. The preceding data indicate that a true anomaly of about 28.9 deg is better than 0 deg.

The lunar anomalistic month accounts for the length of the short-period variations that occur in the escape velocity, but the longer-term envelope variation with a period of 206 days has not yet been linked to a physical phenomenon. One avenue to explore is the drift rate of the lunar perigee. However, the longitude of perigee drifts at a rate of 0.11140354 deg/day, or with a period of 3231 days (Ref. 7). When other related phenomena are explored, it appears that no single parameter has a period near 206 days.

Another possibility is that this rate is some combination of two or more periods. The formula for synodic periods can be used[9]:

$$1/S = (1/T_1) - (1/T_2) \qquad (9)$$

where S is the synodic period and T_1 and T_2 are periods of two different cyclical entities.

When the solar year is used for T_1 (365.25 days) and the lunar perigee drift period for T_2 (3231.495 days), the synodic period S becomes 411.79 days. This is not the 206-day period that is being sought, but if this relationship causes two variations per cycle, the variations would be half of 411.79 days or 205.90 days. This now matches the 206-day period that is being sought and is a possible explanation of the variations.

A physical analysis would help in understanding this in more detail and provide confidence that this is really the source of the variation. From Eq. (5), the lower envelope equation, and the best-fit parameters, the lower boundary has a minimum at $\cos[(d + P_l)2\pi/T_l] = -1$. Thus,

$$d_{\text{min}} = 96.50415315 + 206.0121929k \qquad (10)$$

where d_{min} is the number of elapsed days, from 0000 hrs, 1 January 1998, of the minimum values.

Now that the date on which the minimum occurs has been found, the direction of the sun and the lunar perigee direction can be computed from equations in Ref. 7.

From the difference column of Table 1, note that the minima occur when the perigee direction of the lunar orbit is close to the same direction as the sun, or about 180 deg away. Figure 8 shows the configuration.

From Fig. 8, note that on days 96.5 and 302.5, the lunar line of apsides is in line with the sun, and these dates correspond to minima in the lower envelope fluctuations. On day 198, the lower envelope experiences a maximum, and the sun's direction is at a right angle to the lunar line of apsides.

The conclusion is that for this arrival at 100 km above the surface of the moon, it is more efficient to arrive at the moon when the line of apsides is in line with the sun. To arrive at the moon in the most efficient manner possible, this is combined with the conditions of the short-period minimum. Hence, the best time to arrive is when the lunar line of apsides is in line with the sun and the moon has a true anomaly of 28.9 deg with respect to the Earth.

Table 1 Lunar perigee compared to mean solar longitude

d_{min}, days	Mean longitude of lunar perigee, deg	Mean longitude of the sun, deg	Difference, deg
96.50415	12.72407	15.56968	2.845602
302.5163	35.67456	218.625	182.9504
508.5285	58.62505	61.68028	3.055227
714.5407	81.57554	264.7356	183.16
920.5529	104.526	107.7909	3.264852

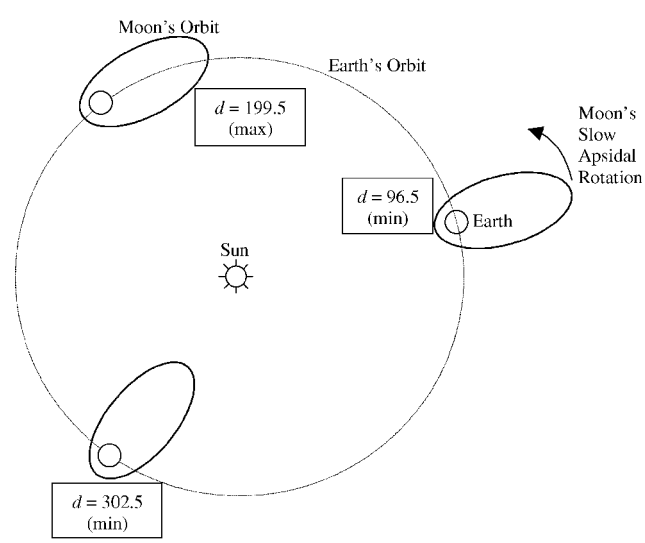

Fig. 8 Envelope variations.

To investigate how these parameters change in relation to changes in the perilune altitude, several more trials were run. The results are in Table 2.

The amplitudes and biases change, but the periodic and phase offset parameters remain effectively the same for all of the perilune altitudes. This means that although the velocities change for the different altitudes, the optimal arrival conditions described apply regardless of the perilune altitude.

Notice that, between the best and worst cases (Fig. 6), there is only a 5-m/s difference. Therefore, the time of arrival is not a big factor in efficiency. However, when the exact velocity of a BCT is looked for, these velocity oscillations provide a very good first estimate.

Lunar Ballistic Capture Trajectory Conditions

When the escape velocities in Fig. 6 are compared to the velocities that actually result in BCT trajectories (Fig. 9), note that they are very close to being the same, but that there are some added variations to the sinusoidal wave.

To better see how much different the BCT velocities are from the escape velocities, the two values are differenced at each time point. Figure 10 shows the result of this differencing for a time span of 750 days, instead of the almost 1500 days, to display the details better.

Table 2 Envelope parameters for various perilune altitudes

	Altitude, km				
Parameter	100	500	1000	2000	5000
A_u, km/s	0.000372	0.000417	0.00046	0.000531	0.000646
A_l, km/s	0.000387	0.000435	0.000486	0.000581	0.000756
P_u, days	109.5089	108.7357	109.2754	109.6942	108.1331
T_u, T_l, days	206.0124	206.0153	206.0572	206.1536	206.0769
B_u, km/s	2.269081	2.048322	1.842866	1.561926	1.13025
B_l, km/s	2.264848	2.04368	1.837757	1.556012	1.122586
P_s, days	7.815455	7.799149	7.764592	7.719022	7.556663
T_s, days	27.55834	27.55804	27.5577	27.55782	27.55834

Although the differences are very small, the results exhibit a repeating pattern of curves with an approximately exponential decay. The period is on the order of 14.7 days. If this number is doubled, the result is 29.4 days, which corresponds with the synodic lunar month of 29.530589 days (new moon to new moon).[7] This indicates that the velocity needed in addition to the actual escape velocity is not dependent on the perigee of the moon, as is the escape velocity, but is tied to the relation of the sun's position with respect to the Earth and the moon. It appears that, over the course of the lunar synodic month, the pattern repeats twice.

Because the sun appears to play a large part in this, Fig. 11 shows the extra velocity needed vs the SEM angle at lunar departure. It shows that there is a definite repeating pattern that does correlate strongly with the SEM configuration. Near the −70- and 110-deg SEM angles, it appears that there may be more than one trajectory that can be taken to achieve a BCT from this family.

Through the use of Fig. 10 and the escape velocity equation (3), a good initial estimate can be made for the velocity needed to leave the moon on a BCT trajectory. The values obtained could be incorporated into a search algorithm for BCTs as very good initial guesses. This could help accelerate a BCT search process significantly. The values given here are for the specific lunar altitude of 100 km and an ecliptic inclination of 0 deg, along with the altitude of 200 km at Earth.

The same analysis was completed for BCTs with several perilune altitudes. Each altitude resulted in the pattern shown in Fig. 12, with repetitions occurring with the same period and with variations in velocity of up to 2 m/s, as is seen in the 100-km altitude case.

These patterns could be used as a starting point in a search algorithm to find BCTs. More importantly though, this section has shown the basic properties of the arrival/escape velocities and how the various components relate to Earth–moon conditions and SEM conditions.

Lunar Arrival Eccentricity

Because the radius of perilune is fixed for each case, the eccentricity of the orbit at perilune can be directly related to the value of the

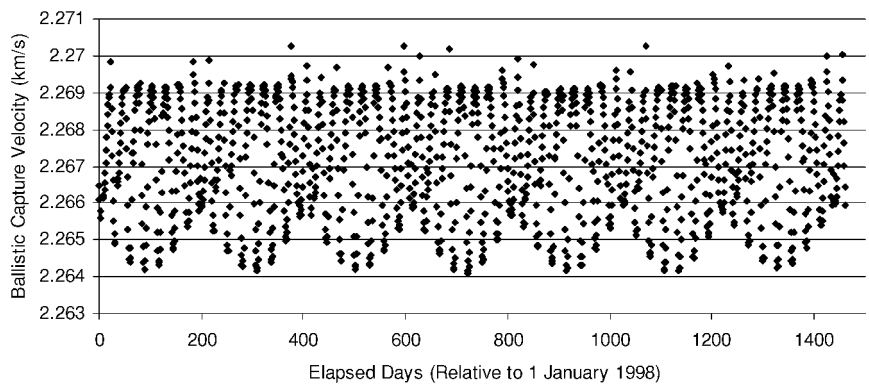

Fig. 9 Ballistic capture velocities at the moon.

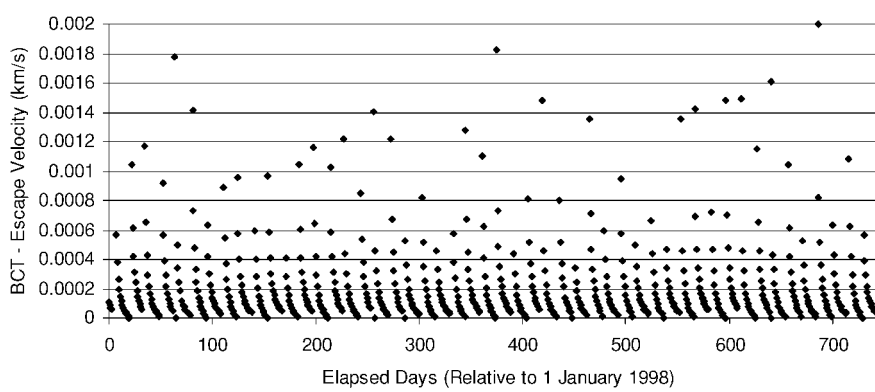

Fig. 10 Extra velocity beyond escape velocity needed for BCT.

velocity. Note from Fig. 9 that the minimum and maximum velocities of the BCTs are roughly 2.264 and 2.270 km/s. The eccentricity range can be found with the following relationships:

$$e = 1 - (r_p/a), \qquad a = (-\mu_m/2\varepsilon)$$

$$\varepsilon = (v^2/2) - (\mu_m/r) \tag{11}$$

where e is the eccentricity of the orbit, r_p is the radius of periapsis (1838 km in this case), a is the semimajor axis of the orbit, ε is the specific mechanical energy of the orbit, v is the velocity of the spacecraft, μ_m is the gravitational parameter (4902.8 km^3/s^2 in this case), and r is the magnitude of the position vector (also 1838 km in this case).

With the preceding minimum and maximum velocities, the resulting eccentricities are 0.92 and 0.93, respectively. This means that, for BCT trajectories, this is the range of values the satellite will have at perilune, without the need for any ΔV at perilune to be captured. Table 3 lists eccentricity values for other perilune altitudes.

Lunar Arrival Dates

BCTs have been found for many time points when work begins at the moon and is then performed backward in time. At each time point, the initial conditions are established and the eccentricity is varied in search of a BCT. The search algorithm either returns the necessary velocity, or it returns a velocity of zero if no BCT is found. Figure 12 contains the results from a one-year search time span with one-day increments between each initial condition epoch.

Table 3 Eccentricity ranges for captures at various perilune altitudes

	Altitude, km				
Eccentricity	100	500	1000	2000	5000
Minimum	0.92	0.91	0.89	0.85	0.73
Maximum	0.93	0.92	0.90	0.86	0.76

Spikes that drop down to zero indicate that no BCT solution was found by the program for that time point. These happen approximately 14.5 days apart, which again is indicative of one-half of a lunar synodic month. Hence, certain conditions with respect to the sun appear to make some time periods less conducive to supporting BCTs. However, Fig. 12 does show that there are some cycles where BCTs are found where sun conditions are not normally favorable; such time periods are near days 97, 128, 158, and 349.

Figure 13 displays the same data as Fig. 12, except that they are now plotted against the SEM angle instead of elapsed days.

Note from these data that problems are sometimes encountered when an attempt is made to find solutions in the regions around −110 to −55 deg and 75 to 120 deg. However, it can also be seen that many solutions are found in these regions too, and so BCT trajectories are possible in these conditions even if they are not possible in every instance. Note that these are the same regions where two potential solutions are theorized based on Fig. 11.

Lunar Orbit Stability

The BCTs do not need a second ΔV to enter an elliptic orbit around the moon. However, these elliptic capture orbits are not stable and, over a period of time, will eventually result in the spacecraft escaping the moon again unless a burn is performed to reduce the spacecraft's energy to a level in which it will stay in lunar orbit for a longer time.

The natural question that follows deals with how long the spacecraft will stay in orbit around the moon until it escapes again. Figure 14 contains the answer for the 100-km lunar perilune altitude case. For Fig. 14, the spacecraft is propagated forward from perilune until the energy of the orbit with respect to the moon becomes positive. The length of time for this condition to occur is then recorded.

The length of time that the spacecraft stays in orbit varies from a region of around 17 days, then switches to a region of around 8 days, and then repeats the cycle. Between each transition from 17 to 8 days, or back again, a spike is produced where the spacecraft

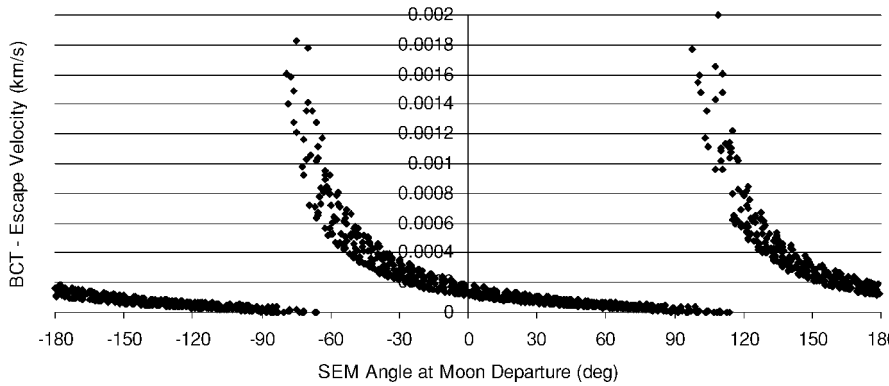

Fig. 11 BCT, escape velocity vs SEM angle at moon departure.

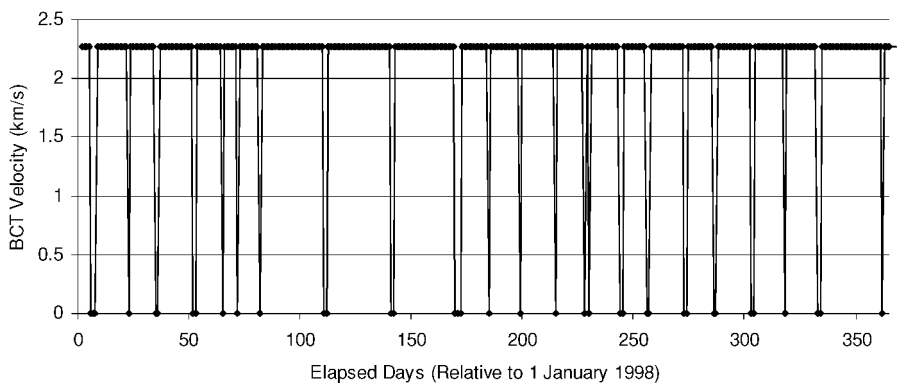

Fig. 12 Lunar arrival dates that generate BCT solutions (velocity of zero indicates that no BCT is possible).

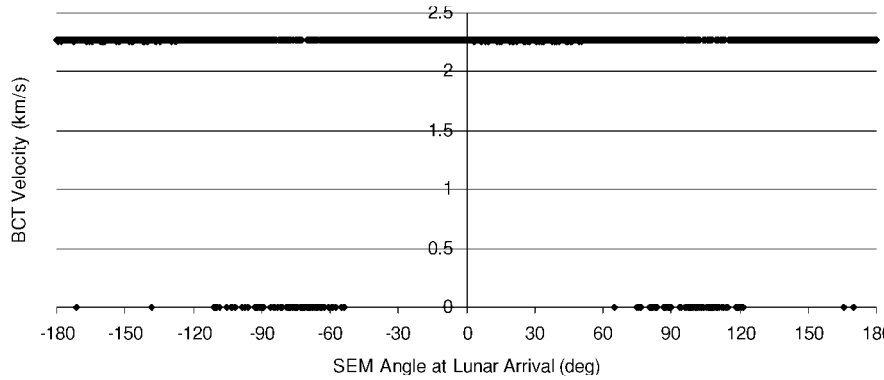

Fig. 13 Lunar arrival SEM angles that do not generate BCT solutions.

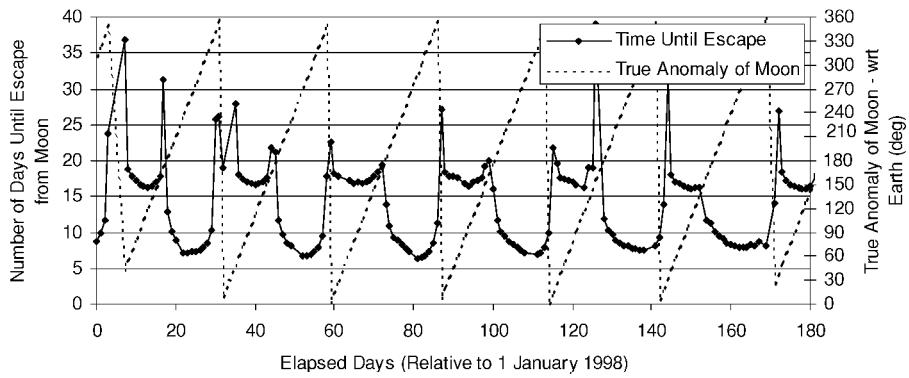

Fig. 14 Lunar orbit stability.

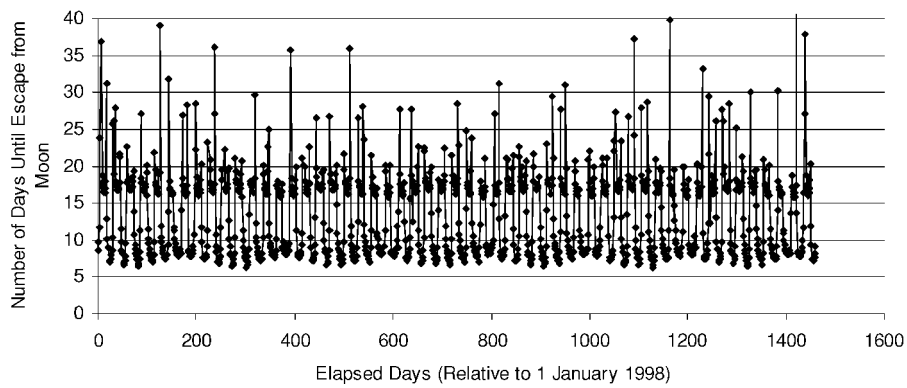

Fig. 15 Lunar orbit stability over four-year time span.

may stay in orbit for much longer. Although not shown in Fig. 14, one such case remained in orbit for 74 days before escaping the moon.

The cycling between 17- and 8-day regions happens roughly every 27.5 days, and so, again, it appears that the cycle period may be related to the lunar anomalistic month (perigee to perigee), which is 27.55455 days. When Eq. (7) is used to overlay a plot of the moon's true anomaly in Fig. 14, note that there is a close correlation between the 17- and 8-day regions compared to the true anomaly. If a spacecraft arrives when the moon is traveling from perigee to apogee, it will stay captured for around 17 days. If a spacecraft arrives when the moon is traveling from apogee to perigee, it will stay captured for only around 8 days. However, if the spacecraft arrives when the moon is at its perigee or apogee, capture times can be much longer.

Figure 15 includes the same capture stability data as Fig. 12, except that these data show the variations over a four-year period instead of just 180 days.

The 17- and 8-day regions do not appear to have any secular variations; however, there are obviously small periodic variations. These variations correspond with the long-term variations seen in the escape velocity (Fig. 6).

Again, the capture stability analysis was performed on perilune altitudes other that 100 km, and the patterns are almost identical to the 100-km altitude case shown in Figs. 14 and 15. However, at the transition regions near the moon's perigee and apogee, the capture times get longer for higher perilune altitudes.

Conclusions

When work is performed backward in time from a perilune position, the escape velocity variations for a given altitude are mainly a function of the moon's true anomaly. The minimum-sized escape maneuver occurs when the moon has a true anomaly of approximately 29 deg with respect to the sun. Smaller variations are also evident that depend on the sun's location with respect to the moon's line of apsides. To pick the most efficient condition for this variation, the escape should occur when the line of apsides lines up with the sun. Also note that, whereas the escape velocity depends mainly on the true anomaly of the moon with respect to the Earth, the extra

velocity needed to obtain a BCT trajectory depends on the relative position of the sun.

Other properties found in the analysis are that BCT trajectories reaching the moon with a perilune altitude of 100 km have eccentricities near 0.92–0.93. Also, lunar arrival dates for BCT trajectories can occur on most dates, but there are certain lunar arrivals with SEM configurations (SEM angles) where solutions do not exist or are more difficult to find.

When work is done in a forward time sense, if a BCT arrival occurs when the moon is traveling from its perigee to apogee, the spacecraft is captured for about 17 days after reaching perilune. It remains captured for about 8 days if it arrives when the moon is traveling from apogee to perigee. If lunar arrival occurs at the moon's perigee or apogee, the capture times can be much longer.

References

[1]Sweetser, T. H., "An Estimate of the Global Minimum DV Needed for Earth-Moon Transfer," *Advances in the Astronautical Sciences, Spaceflight Mechanics 1991*, Vol. 75, Pt. 1, Univelt, San Diego, CA, 1991, pp. 111–120.

[2]Yamakawa, H., Kawaguchi, J., Ishii, N., and Matsuo, H., "A Numerical Study of Gravitational Capture Orbit in the Earth–Moon System," *Advances in the Astronautical Sciences, Spaceflight Mechanics 1992*, Vol. 79, Pt. 1, Univelt, San Diego, CA, 1992, pp. 1113–1132.

[3]Belbruno, E. A., and Miller, J. K., "Sun-Perturbed Earth-to-Moon Transfers with Ballistic Capture," *Journal of Guidance, Control, and Dynamics*, Vol. 16, No. 4, 1993, pp. 770–775.

[4]Dahlke, S. R., "Investigation of Lunar Ballistic Capture Transfer Trajectories," Ph.D. Dissertation, Dept. of Aerospace Engineering Sciences, Univ. of Colorado, Boulder, CO, Dec. 1998.

[5]Yamakawa, H., Kawaguchi, J., Ishii, N., and Matsuo, H., "Applicability of Ballistic Capture to Lunar/Planetary Exploration," 1st Workshop on Missions for Planetary Exploration, Kusatsu, Japan, Jan. 1993 (unpublished).

[6]Neto, E. V., and Prado, A. F. B. D., "A Study of the Gravitational Capture in the Restricted-Problem," NASA N96-22127, 1995.

[7]*The Astronomical Almanac*, Nautical Almanac Office, U.S. Government Printing Office, 1998, pp. D1–D46.

[8]Neto, E. V., and Prado, A. F. B. D., "Study of the Gravitational Capture in the Elliptical Restricted Three-Body Problem," NASA N99-10008, May 1996.

[9]Roy, A. E., *Orbital Motion*, Adam Hilger, Bristol, England, U.K., 1991, p. 384.